Preparation and Properties of Nylon 6/Carboxylic Silica Nanocomposites via *In Situ* Polymerization

Lala Zhang, Yuzi Xiong, Encai Ou, Zhongming Chen, Yuanqin Xiong, Weijian Xu

Institute of Polymer Science and Engineering, College of Chemistry and Chemical Engineering, Hunan University, Changsha 410082, China

Received 3 August 2010; accepted 14 December 2010
DOI 10.1002/app.33967
Published online 23 May 2011 in Wiley Online Library (wileyonlinelibrary.com).

ABSTRACT: Nylon 6/carboxylic acid-functionalized silica nanoparticles (SiO_2-COOH) nanocomposites were prepared by *in situ* polymerization of caprolactam in the presence of SiO_2-COOH. The aim of this work was to study the effect of carboxylic silica on the properties of the nylon 6 through the interfacial interactions between the SiO_2-COOH nanoparticles and the nylon 6 matrix. For comparison, pure nylon 6, nylon 6/SiO_2 (unmodified) and nylon 6/amino-functionalized SiO_2 (SiO_2-NH_2) were also prepared via the same method. Fourier transform infrared spectrometer (FTIR) spectroscopy was used to evaluate the structure of SiO_2-COOH and nylon 6/SiO_2-COOH. The results from thermal gravimetric analysis (TGA) indicated that decomposition temperatures of nylon 6/SiO_2-COOH nanocomposites at the 5 wt % of the total weight loss were higher than the pure nylon 6. Differential scanning calorimeter (DSC) studies showed that the melting point (T_m) and degree of crystallinity (X_c) of nylon 6/SiO_2-COOH were lower than the pure nylon 6. Mechanical properties results of the nanocomposites showed that nylon 6 with incorporation of SiO_2-COOH had better mechanical properties than that of pure nylon 6, nylon 6/SiO_2, and nylon 6/SiO_2-NH_2. The morphology of SiO_2, SiO_2-NH_2, and SiO_2-COOH nanoparticles in nylon 6 matrix was observed using SEM measurements. The results revealed that the dispersion of SiO_2-COOH nanoparticles in nylon 6 matrix was better than SiO_2 and SiO_2-NH_2 nanoparticles. © 2011 Wiley Periodicals, Inc. J Appl Polym Sci 122: 1316–1324, 2011

Key words: nylon 6; SiO_2-COOH; nanocomposites; *in situ* polymerization; mechanical properties

INTRODUCTION

Nanoparticles-reinforced polymer nanocomposites are used in many engineering materials because they show a significant improvement in strength and toughness over the native polymer. The success of nanoparticles as reinforcing agents in polymer composites is due to their intrinsic mechanical properties. The incorporation of inorganic particulate fillers has proved to be an effective way to improve the mechanical properties, especially for nylon.[1,2] In recent years, polyamide 6 (nylon 6)/SiO_2 nanocomposites have been paid more and more attention due to their excellent thermal and mechanical properties. The addition of SiO_2 nanoparticles has a significant effect on the thermal and mechanical properties of nylon 6.[2–5] Compared with pristine silica, the incorporation of silane coupling agents modified silica can dramatically improve their mechanical and heat resistance. Consequently, the silica nanoparticles were first treated with 3-aminopropyltrimethoxysilane (APTMS) in our work. Then the surface amino groups could be readily transformed into carboxylic groups by the reaction with succinic anhydride in the presence of triethylamine. The nanoparticles utilized are SiO_2-COOH nanoparticles which are different from SiO_2 and SiO_2-NH_2 nanoparticles, filled in the nylon 6 matrix.

Nylon 6 as a semicrystalline engineering thermoplastic was widely used in the production of nanocomposites that is well-known for its balance of strength, modulus, and chemical resistances. Concerning nylon 6 nanocomposites, a large number of reports have focused on nylon 6/clay nanocomposites prepared by melt blending and intercalation methods resulting in improved mechanical and thermal properties.[6–14] These approaches, however, are only suitable for clay minerals. Cho and Paul[6] made an interesting comparison between *in situ* polymerization and melt-compounding. They concluded that the mechanical properties of *in situ* polymerized nanocomposites are superior to the melt-compounded ones. *In situ* polymerization has been reported by many groups. For example, Gao et al.[15,16] studied the preparation of a single-walled carbon nanotube (SWNT)-nylon 6 composite fiber via *in situ* polymerization. It simultaneously optimizes SWNT-dispersion and enhances the interfacial bonding through covalent grafting between the

Correspondence to: W. Xu (weijianxu_59@163.com).
Contract grant sponsor: Shijiazhuang Chemical Fiber Co., Ltd., China.

polymer chain and the engineered functionality of the SWNTs. It also allows the resulting material to be spun into fibers with arbitrary length. Reynaud et al.[17] prepared nanocomposites consisting of nanoscopic silica fillers embedded in nylon 6 through *in situ* polymerization. The silica in nylon 6 matrix dispersed homogeneously and the obtained materials showed good mechanical properties. Yang et al.[18] studied the preparation of nylon 6/silica nanocomposites through *in situ* polymerization. The results showed that the silica homogeneously dispersed in the nylon 6 matrix. Therefore, nylon 6/SiO_2-COOH nanocomposites were synthesized by *in situ* polymerization. To sum up, nanoparticles can evenly disperse in the polymer matrix by *in situ* polymerization and the obtained nanocomposites have good processing properties.

In this article, SiO_2-COOH nanoparticles were synthesized and nylon 6/SiO_2-COOH nanocomposites were prepared via *in situ* polymerization of caprolactam. The objective of this work is to study the effect of SiO_2-COOH nanoparticles on the properties of nylon 6/SiO_2-COOH nanocomposites. To the best of our knowledge, no work about the preparation of nylon 6/SiO_2-COOH nanocomposites by *in situ* polymerization of caprolactam can be found. The nylon 6/SiO_2-COOH nanocomposites were characterized by FTIR, TGA, DSC, SEM, and mechanical properties tests. Meanwhile, pure nylon 6, nylon 6/SiO_2, and nylon 6/SiO_2-NH_2 were also investigated.

EXPERIMENTAL

Material

Triethylamine (TEA), succinic anhydride, and 3-aminopropyltrimethoxysilane (APTMS) were purchased from Shanghai Reagents Company. ε-Caprolactam was friendly supplied by Baling Petrochemical (Yue Yang, China). Nano-SiO_2 (50 nm) was purchased from Shenzhen Duocai. Toluene was distilled under atmospheric pressure before use. N, *N*-dimethylformamide (DMF) and anhydrous ethanol were analytical grade without further purification.

Preparation of amino-functionalized silica nanoparticles (1), carboxylic acid-functionalized silica nanoparticles (2), and nylon 6/SiO_2-COOH nanocomposites by *in-situ* polymerization (3)

(1) Amino-functionalized silica nanoparticles (SiO_2-NH_2) were prepared according to the procedures described in the literature.[19] In a typical procedure, 3.3 mL APTMS was added to a mixture of 3.87 g silica nanoparticles and 100 mL anhydrous toluene, and the mixture was stirred under nitrogen at 90°C for 24 h. The nanoparticles were washed by centrifugation and redispersed in toluene. Above procedure was repeated three times. (2) Carboxylic acid-functionalized silica nanoparticles (SiO_2-COOH): typically, 1 g SiO_2-NH_2 was dispersed in DMF (50 mL) in a flask. Then 0.5 g succinic anhydride and 5 mL triethylamine (TEA) were added to the flask. The mixture was stirred under nitrogen at 70°C for 20 h. The resulting silica nanoparticles with carboxylic-function groups at their surface (SiO_2-COOH) were washed as described earlier. DMF was used as the washing medium. (3) Nylon 6/SiO_2-COOH nanocomposites: typically, ε-caprolactam (500 g), distilled water (10 g), and SiO_2-COOH (1 g) were added to 2-L autoclave. The autoclave was then placed under vacuum and crushed with high-purity nitrogen thrice to remove any air. Then, the temperature was elevated from room temperature to 215°C over a period of about 40 min with stirring. The process of ε-caprolactam hydrolysis ring-opening and prepolymerization went on for 2 h. Then, the temperature was elevated to 265°C over 25 min, the process of polymerization took 4 h. After that, the inner temperature was cooled to about 230°C, and the autoclave was opened from a bottom valve. The production was drawn into long strands in a water bath and then pelletized with scissors. Whereafter, the final products were extracted in boiled water for 20 h, and dried under vacuum at 100°C overnight. Sample nylon 6/SiO_2-COOH containing 0.2 wt % of SiO_2-COOH units was then obtained.

Characterization

FTIR spectra were recorded on a WQF-410 FTIR spectrometer using potassium bromide (KBr) discs prepared from powdered samples mixed with dry KBr. The thermal stability of the samples (about 7 mg) was investigated with a thermal gravimetric analyzer (TGA, a Netzsch STA 449C), each sample was first heated from 30 to 100°C at a rate of 10°C/min and maintained at 100°C for a period of 5 min, then cooled down to 60°C at the same rate, after that heated again from 60 to 800°C with a rate of 10°C/min. Differential scanning calorimetry analysis was carried out with a Netzsch STA 204C modulated DSC system. All samples were first heated from room temperature to 250°C at a rate of 10°C/min and maintained at 250°C for a period of 5 min, then cooled down to 50°C at the same rate, after that heated again from 50 to 300°C with a rate of 10°C/min. All samples for mechanical tests were injection-molded in an injection-molding machine (GEK-80, Zhejiang Golden Eagle Plastic Machinery, China). The tensile strength, Young's modulus, and elongation at break were tested on a universal testing machine (WDW 3020 Changchun Branch new Experimental Instrument, China) at room temperature with the speed of 50 mm/min according to GB/T

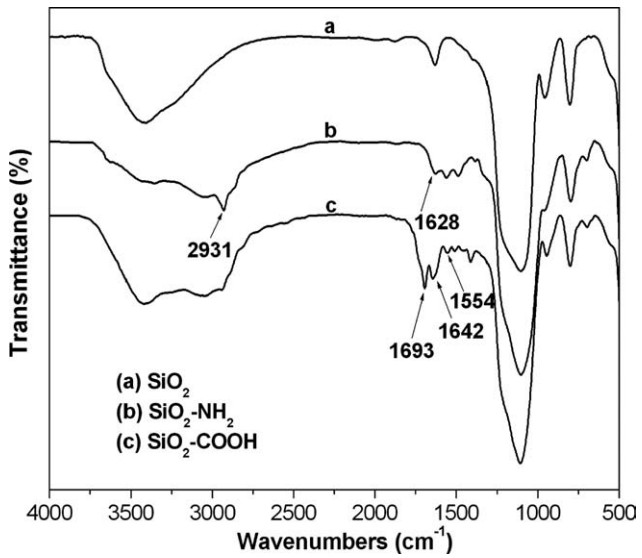

Figure 1 FTIR spectra of original SiO_2 (a), SiO_2-NH_2 (b), and SiO_2-COOH (c).

16421-1996 (China). The Izod impact strength was measured according to GB/T 1043-93 (China). The bending test was carried out according to GB/T 9341-2000 (China) at the crosshead speed of 2 mm/min. All tests were done at room temperature, and average value of at least five times was reported. A field emission scanning electron microscope (FE-SEM, Hitachi S4800) was used to observe the fractured morphology of pure nylon 6 and nanocomposites after Izod impact testing. Fractured surfaces were coated with gold in an SPI sputter coater. The morphology was determined using an accelerating voltage of 5.0 kV.

RESULTS AND DISCUSSIONS

Synthesis and characterization of SiO_2—NH_2 and SiO_2—COOH

With the purpose of removing the impurities, silica nanoparticles were soaked in aqueous solution of hydrochloric acid for 2 days before use. After that, silica nanoparticles were converted into amino-terminated silica nanoparticles (SiO_2-NH_2) by reaction with APTMS. The amino groups on the SiO_2 surface (SiO_2-NH_2) reacted with succinic anhydride was introduced to prepare the SiO_2-COOH.[20] The conversion was effectively tested by adding salicylaldehyde. Upon addition of salicylaldehyde, SiO_2-NH_2 turned yellow immediately, indicating the presence of amino groups, whereas SiO_2-COOH was hardly observed yellow even after 24 h. This is a clear indication that most of the amino groups have reacted.[19]

The FTIR spectra of pristine SiO_2 and functionalized SiO_2 are shown in Figure 1. Compared with pristine SiO_2, there are several new peaks appearing in the spectra of SiO_2-NH_2 and SiO_2-COOH. For the SiO_2-NH_2, the stretching vibration of the C—H bond occurs at 2931 cm^{-1}, and the bending vibration of the *N*—H bond appears at 1628 cm^{-1}. This indicates successful grafting of APTMS to the surface of SiO_2. For the SiO_2-COOH, the band at 1693 cm^{-1} corresponds to the stretching vibration of the C=O group of the carboxylic acid functionality in SiO_2-COOH. The stretching vibration of the C=O group of amide functionality in SiO_2-COOH occurs at 1642 cm^{-1}. The band at 1554 cm^{-1} corresponds to a combination of the bending vibration of the *N*—H bond and the stretching vibration of C—N bond of the amide group.[21] Thus, FTIR analysis suggests the successful formation of SiO_2-COOH.

Figure 2 showed the weight loss curves of SiO_2, SiO_2-NH_2, and SiO_2-COOH. From the TGA curves, only 4.5 wt % of weight loss was found for SiO_2 below 600°C. There were two main temperature regions of weight loss. The weight loss below 460°C could be attributed to the evaporation of physical absorbed water and residual solvent in the samples. The weight loss in the temperature beyond 460°C could be assigned to the decomposition of silica-bonded groups such as —OH.[22] For SiO_2-NH_2, 18.6 wt % of weight loss was detected between 200 and 600°C, indicated that APTMS were successfully grafted to the surface of SiO_2. Correspondingly, the amino density of SiO_2-NH_2 was calculated according to the following equation[23]:

$$\frac{100\% - 4.5\%}{100\% - 18.6\%} = \frac{4.5\%}{X} \Rightarrow X = 3.84\%$$

$$\frac{18.6\% - 3.84\%}{M} = 2.54\text{mmol/g}$$

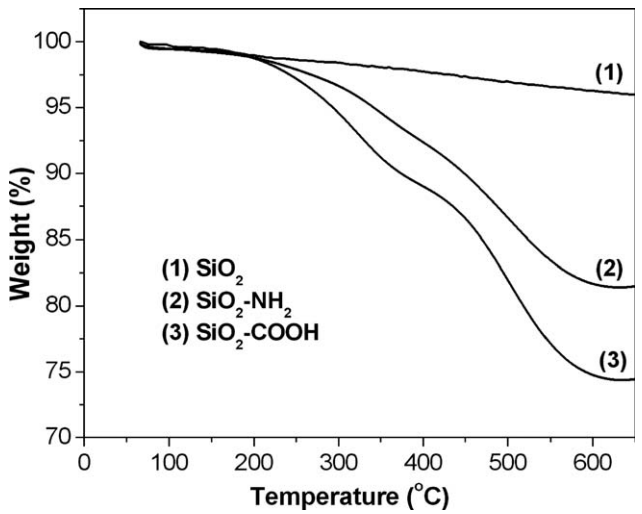

Figure 2 TGA curves obtained from SiO_2 (a), SiO_2-NH_2 (b), and SiO_2-COOH (c).

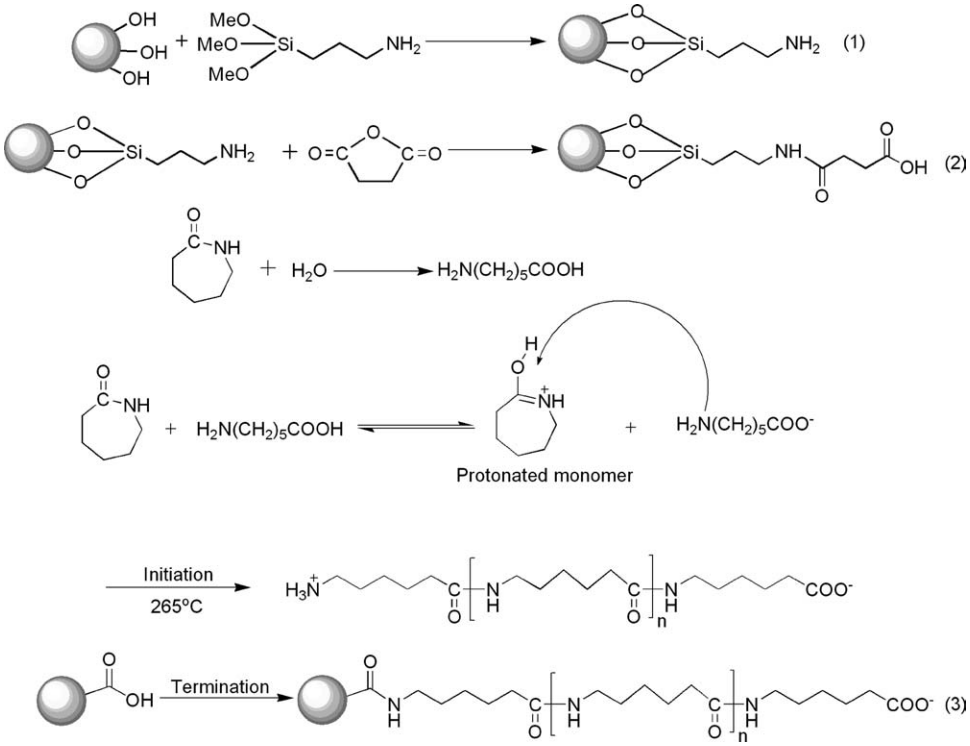

Scheme 1 The synthesis process of nylon 6/SiO_2-COOH.

where 4.5% was the weight loss of the evaporation of physical absorbed water, residual solvent, and decomposition of silica-bonded groups such as —OH of SiO_2. 18.6% was the weight loss of the evaporation of physical absorbed water, residual solvent, decomposition of silica-bonded groups such as —OH and organic molecular chain of SiO_2-NH_2. X was the weight loss of the evaporation of physical absorbed water, residual solvent, and decomposition of silica-bonded groups such as —OH of SiO_2-NH_2. M was the molecular weight of APTMS grafted to the SiO_2-NH_2. Here, the calculated value of M of SiO_2-NH_2 was 58 g/mol. For SiO_2-COOH, its weight loss between 200 and 600°C increased to 25.8 wt %, corresponding to the density of 1.41 mmol/g of carboxylic groups on the periphery of SiO_2 with the same method. It demonstrated further derivative reaction of SiO_2-NH_2 was carried out by succinic anhydride.

Synthetic process of nylon 6/SiO_2—COOH nanocomposites and FTIR analysis

Nylon 6/SiO_2-COOH nanocomposites were synthesized with suitable quantity of SiO_2-COOH, ε-caprolactam, and distilled water by *in situ* ring-opening polymerization. Scheme 1 illustrates the synthetic process of nylon 6/SiO_2-COOH nanocomposites. During the synthesis of nanocomposites, the ring-opening polymerization of caprolactam proceeds mainly through the amino terminal groups of nylon 6.[24–29] Condensation reaction between the carboxylic-acid groups on the SiO_2 surface and the amino end groups of nylon 6 terminates the chain propagation and results in the formation of nylon 6/SiO_2-COOH.[30] Figure 3 shows the detailed FTIR spectra of pure nylon 6 and nylon 6/SiO_2-COOH nanocomposites. The nylon 6/SiO_2-COOH nanocomposites have similar spectra as pure nylon 6. The carbonyl bond (C=O) occurs at 1641 cm^{-1}, and the same

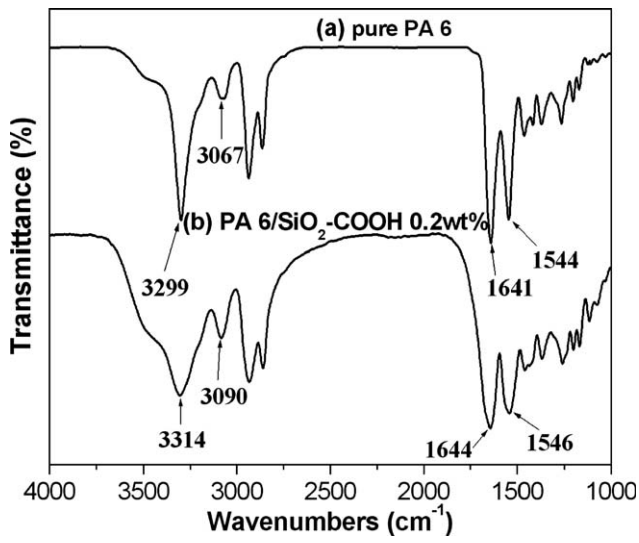

Figure 3 FTIR spectra of pure nylon 6 (a) and nylon 6/SiO_2-COOH 0.2 wt % (b).

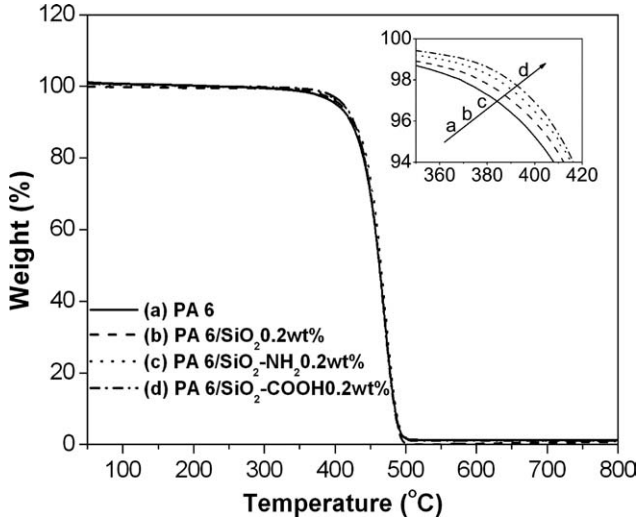

Figure 4 TGA curves of pure nylon 6 (a), nylon 6/0.2 wt % SiO_2 (b), nylon 6/0.2 wt % SiO_2-NH_2 (c), and nylon 6/0.2 wt % SiO_2-COOH (d).

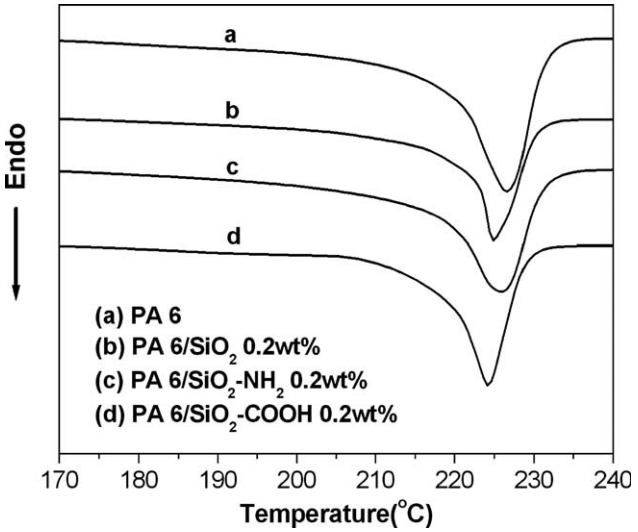

Figure 5 DSC heating curves of pure nylon 6 (a), nylon 6/0.2 wt % SiO_2 (b), nylon 6/0.2 wt % SiO_2-NH_2 (c), and nylon 6/0.2 wt % SiO_2-COOH (d).

features also occur at 1544 cm^{-1} (the bending vibration of *N*—H bond and the stretching vibration of C—N bond). The differences occur at 3314 and 3299 cm^{-1} (the dissymmetrical stretching vibration of *N*—H bond), 3090 and 3067 cm^{-1} (the symmetrical stretching vibration of *N*—H). Blue shifts are found for the peaks of *N*—H bond of the nylon 6/SiO_2-COOH nanocomposites compared with the pure nylon 6 in the FTIR spectra, which may be ascribed to the facts that the low loadings of SiO_2-COOH units in nylon 6 matrix disturb the hydrogen bonds between the neighboring molecular chains.[31] Moreover, the peaks of *N*—H and C=O bonds of the amide functionality in the nylon 6/SiO_2-COOH nanocomposites are broader than that of pure nylon 6, which may be due to the reaction between the carboxylic-acid groups on the SiO_2 surface and the amino end groups of the nylon 6. It is believed that the increase in the bond strength of *N*—H and C=O functional groups are induced by the presence of SiO_2-COOH nanoparticles, indicating that the nylon 6 chains have grafted onto the SiO_2.

TGA of nylon 6 and its nanocomposites

Figure 4 shows the TGA curves of pure nylon 6, nylon 6/SiO_2, nylon 6/SiO_2-NH_2, and nylon 6/SiO_2-COOH. It can be observed that the thermogravimetic curves of nylon 6/SiO_2 (0.2 wt %), nylon 6/SiO_2-NH_2 (0.2 wt %), and nylon 6/SiO_2-COOH (0.2 wt %) nanocomposites are similar to the pure nylon 6. The decomposition temperature is defined as the temperature at the 5% of the total weight loss. Therefore, the decomposition temperatures for pure nylon 6, nylon 6/SiO_2 (0.2 wt %), nylon 6/SiO_2-NH_2 (0.2 wt %), and nylon 6/SiO_2-COOH (0.2 wt %) are 401, 406, 409, and 412°C, respectively, suggesting that the thermal stability of nylon 6/SiO_2, nylon 6/SiO_2-NH_2 nanocomposites slight increase compared with that of pure nylon 6. However, the decomposition temperatures of the nylon 6/SiO_2-COOH nanocomposites seemed to have been increased by 11°C. This demonstrated that the nylon 6/SiO_2-COOH nanocomposites were thermally more stable than pure nylon 6 and other nanocomposites, which might be due to the facts that there were the presence of very strong interfacial interactions between SiO_2-COOH nanoparticles and nylon 6 matrix.

DSC of nylon 6 and its nanocomposites

Figure 5 shows the DSC heating curves of pure nylon 6 and various nanocomposites. Values of melting point (T_m) and degree of crystallinity (X_c), as determined from Figure 5, are shown in Table I. It is observed that there is a slight decrease in the melting point and degree of crystallinity of nanocomposites compared with pure nylon 6. In Refs. [32–34] they also showed that T_m and X_c of nylon 6 slight decreased when the nylon 6 was filled with colloidal silica with a particle size of about 10–20 nm.

TABLE I
Summarization of the Data Obtained From DSC Test

Samples	T_m (°C)	X_c (%)	ΔH_f (J/g)	T_c (°C)
Nylon 6	226.8	29.8	68.59	187.4
Nylon 6/SiO_2	225.5	22.5	51.71	186.5
Nylon 6/SiO_2-NH_2	224.8	23.1	53.12	183.1
Nylon 6/SiO_2-COOH	223.8	24.7	56.80	186.9

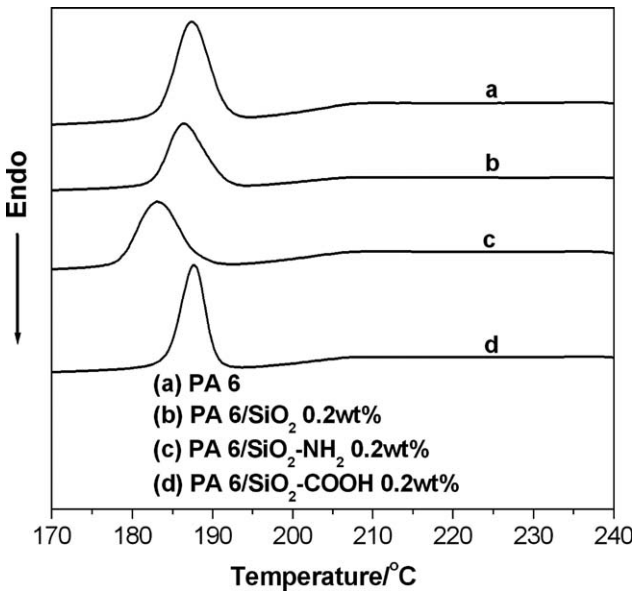

Figure 6 DSC cooling curves of pure nylon 6 (a), nylon 6/0.2 wt % SiO_2 (b), nylon 6/0.2 wt % SiO_2-NH_2 (c), and nylon 6/0.2 wt % SiO_2-COOH (d).

Whereas, the small differences of X_c among the various nanocomposites cannot have a distinct influence on the differences of mechanical property of the final materials. Furthermore, nylon 6/SiO_2-COOH nanocomposites display lower melting point than nylon 6/SiO_2 and nylon 6/SiO_2-NH_2 nanocomposites, which may be attributed to the facts that there are more flexible interphase layer existing the interface between the SiO_2-COOH and nylon 6 matrix than that of SiO_2 and SiO_2-NH_2 with nylon 6 matrix.[5] So it is further believed that SiO_2-COOH nanoparticles possess a better miscibility than that of SiO_2 and SiO_2-NH_2 with nylon 6.

To further interpret the decrease in crystallinity, DSC cooling curves are shown in Figure 6. The crystallization temperatures, as determined from Figure 6, are listed in Table I. It is seen in Figure 6 that the crystallization temperatures of the nanocomposites are lower than that of pure nylon 6. Interestingly, the crystallization temperature of PA 6/SiO_2-COOH was bigger than that of PA 6/SiO_2 and PA 6/SiO_2-NH_2, and exhibited the smallest temperature difference compared with pure nylon 6. It can be explained that a more crystalline material would tend to achieve crystalline form at an earlier stage compared with the corresponding less crystalline material during the cooling process.[3] These results were ascribed to good interfacial interaction between the nanoparticles and the polymer and degree of crystallinity.[35] It also indicates that SiO_2-COOH nanoparticles have a good interfacial interaction with nylon 6 matrix, which is consistent with the discussions about FTIR characterization.

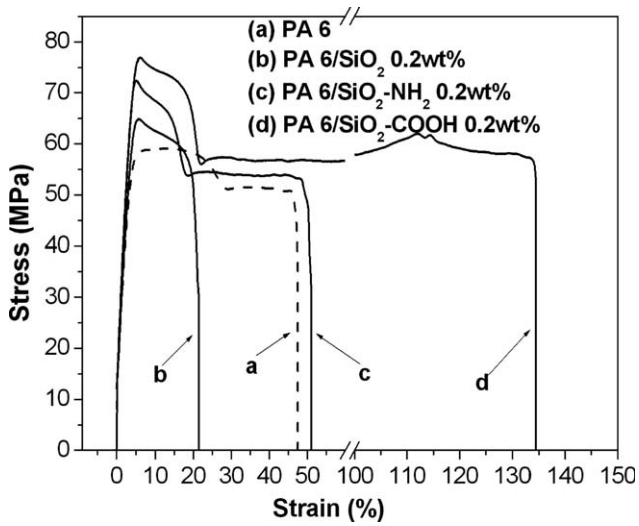

Figure 7 Stress–strain curves of pure nylon 6 (a), nylon 6/0.2 wt % SiO_2 (b), nylon 6/0.2 wt % SiO_2-NH_2 (c), and nylon 6/0.2 wt % SiO_2-COOH (d).

Mechanical properties

Figures 7 and 8 show the representative stress-strain curves from the tensile tests. The results of tensile strength, elongation at break, Izod impact strength, bending strength, and Young's modulus of pure nylon 6, nylon 6/SiO_2, nylon 6/SiO_2-NH_2, and nylon 6/SiO_2-COOH are shown in Table II, respectively. The results of tensile strength, Young's modulus, and elongation at break are obtained from Figures 7 and 8. As shown in Table II, the gain for samples 2, 4, and 6 in Young's modulus is around 7%, 24%, and 27% compared with that of sample 1, respectively. On the other hand, the enhancement for

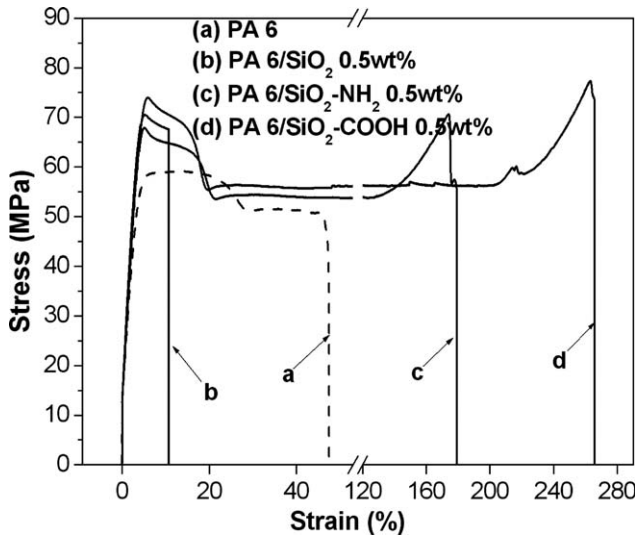

Figure 8 Stress–strain curves of pure nylon 6 (a), nylon 6/0.5 wt % SiO_2 (b), nylon 6/0.5 wt % SiO_2-NH_2 (c), and nylon 6/0.5 wt % SiO_2-COOH (d).

TABLE II
Mechanical Properties of Pure Nylon 6 and Various Nanocomposites

Samples	Tensile strength (Mpa) ± 1	Elongation at break (%) ± 5	Bending strength (Mpa) ± 0.5	Izod impact strength (kJ/m^2) ± 0.2	Young's modulus (Gpa) ± 0.2
Nylon 6 (1)	59.11 (0%)[a]	47.5 (0%)	76.61 (0%)	10.05 (0%)	1.08 (0%)
Nylon 6/SiO_2 0.2 wt %(2)	64.83 (10%)	21.5 (−55%)	79.78 (4%)	13.88 (38%)	1.16 (7%)
Nylon 6/SiO_2 0.5 wt %(3)	70.49 (19%)	10.7 (−77%)	82.11 (7%)	11.75 (17%)	1.21 (12%)
Nylon6/SiO_2-NH_2 0.2 wt %(4)	72.42 (22%)	51.2 (8%)	88.42 (15%)	14.89 (48%)	1.34 (24%)
Nylon 6/SiO_2-NH_2 0.5 wt %(5)	70.61 (19%)	179.5 (278%)	92.15 (20%)	14.69 (46%)	1.27 (18%)
Nylon 6/SiO_2-COOH 0.2 wt %(6)	77.43 (31%)	134.5 (183%)	101.7 (33%)	19.36 (93%)	1.37 (27%)
Nylon 6/SiO_2-COOH 0.5 wt %(7)	77.34 (31%)	265.7 (459%)	92.82 (21%)	16.38 (63%)	1.36 (26%)

[a] Value in parentheses represents percentage increase/decrease as compared to the polymer.

samples 3, 5, and 7 is around 12%, 18%, and 26%, respectively. It can be easily seen that the Young's modulus of nylon 6/SiO_2-COOH nanocomposites are higher than that of the pure nylon 6, nylon 6/SiO_2, and nylon 6/SiO_2-NH_2. This is because that organic molecular chain on the surface of SiO_2-COOH is longer than SiO_2 and SiO_2-NH_2 (see Scheme 1).[5] Thereby, more nylon 6 chains are grafted to the surface of SiO_2-COOH. The formation of amide covalent bonds in the interface between SiO_2-COOH and nylon 6 matrix constitutes the strongest interfacial interaction. Furthermore, it further confirms that SiO_2-COOH nanoparticles display a better compatibility than that of SiO_2-NH_2 with nylon 6 matrix. From Table II, it can also be found that the tensile strength, the bending strength and Izod impact strength of nylon 6/SiO_2-COOH nanocomposites are higher than pure nylon 6, nylon 6/SiO_2, and nylon 6/SiO_2-NH_2. On the other hand, it is obvious that the tensile strength, bending strength, and Izod impact strength of sample 7 are lower than that of sample 6, which may be ascribed to the facts that the introduction of a higher concentration of the carboxylic acid groups on the SiO_2 surface into the reaction medium will consume more amino terminal groups of nylon 6. Hence, this leads to reduce the degree of polymerization, and decrease the average molecular weight of the nylon 6, and weaken the mechanical properties of nylon 6/SiO_2-COOHnanocomposites. In general, the enhancement in strength and toughness can be attributed to the factors as following: (1) the proper dispersion of SiO_2 nanoparticles into the matrix; (2) the development of interfacial bonding between the nanoparticles and the

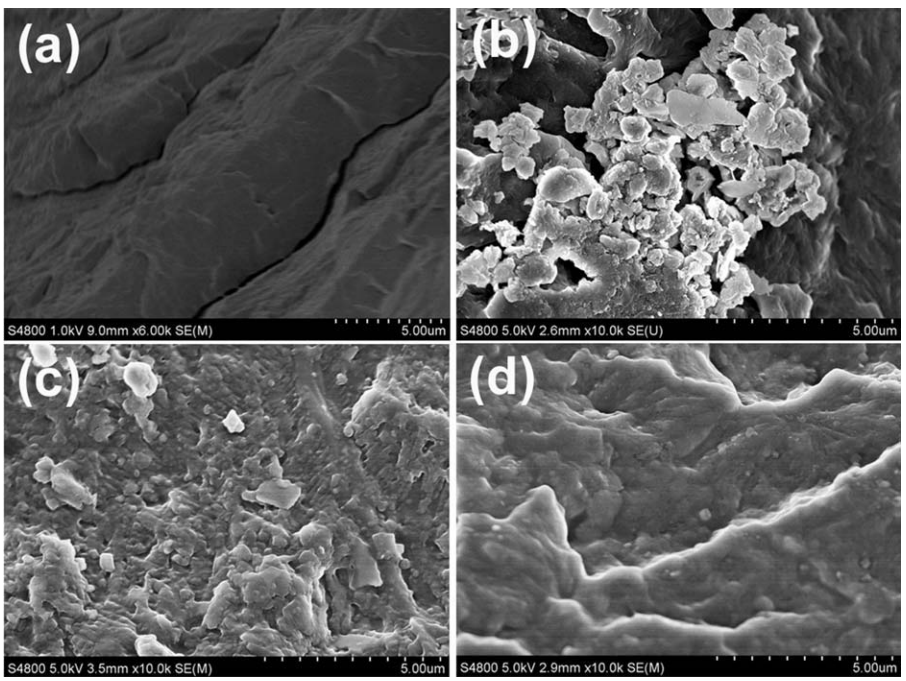

Figure 9 SEM images of pure nylon 6 (a), nylon 6/SiO_2 (b), nylon 6/SiO_2-NH_2 (c), and nylon 6/SiO_2-COOH (d).

polymer[16]; (3) the flexibility of the covalent linkages between the nanoparticles and the polymer chains.[36] From the results given in Table II, it is believed that SiO_2-COOH, with carboxyl groups on its surface, has possible strong interfacial interaction with nylon 6 matrix, thus displays a better miscibility than that of SiO_2 and SiO_2-NH_2 with nylon 6 matrix.

Morphological analysis

To understand why the impact strength of various nanocomposites increased compared with pure nylon 6, the impacted surfaces of pure nylon 6 and various nanocomposites were observed by SEM. Figure 9 shows SEM images of the fracture surfaces of pure nylon 6, nylon 6/SiO_2, nylon 6/SiO_2-NH_2, and nylon 6/SiO_2-COOH. It is clear that images a, b, c, and d exhibit a relatively coarse fracture surface, which indicates that all samples present a typical ductile fracture behavior with some long and big strip-like crack. In addition, image b shows that the unmodified SiO_2 nanoparticles are mostly agglomerated. Image c reveals that some SiO_2-NH_2 particles are agglomerated, while some SiO_2-NH_2 particles are uniformly dispersed over the entire body of the nylon 6 matrix. However, image d displays that SiO_2-COOH nanoparticles are dispersed more uniformly in the nylon 6 matrix than SiO_2 and SiO_2-NH_2 nanoparticles. This improved dispersion can be attributed to the existence of flexible interphase layer introduced by organic molecular chains on the surface of SiO_2-COOH. The SEM analysis is also in accordant with the discussions about the test results of mechanical properties.

CONCLUSIONS

In this study, nylon 6/SiO_2-COOH nanocomposites using SiO_2 bearing carboxylic acid groups on its surface by *in situ* polymerization were synthesized for the first time. FTIR characterization indicates that the nylon 6 chains are found to be grafted to the SiO_2 by a condensation reaction between the carboxylic acid groups on the SiO_2 surface and the amino terminal groups of nylon 6. TGA confirms that nylon 6/SiO_2, nylon 6/SiO_2-NH_2, and nylon 6/SiO_2-COOH nanocomposites are more thermally stable than pure nylon 6. What is more, the decomposition temperature of nylon 6/SiO_2-COOH nanocomposites increases by 11°C compared with that of pure nylon 6. DSC results reveal that the melting points and the degree of crystallinity of the nanocomposites have a slight decrease compared with that of pure nylon 6. The tensile strength, bending strength, Izod impact strength, elongation at break, and Young's modulus of nylon 6/SiO_2-COOH nanocomposites are higher than that of pure nylon 6, nylon 6/SiO_2, and nylon 6/SiO_2-NH_2. Mechanical performance evaluations show that SiO_2 with carboxylic acid groups on its surface can form a stronger SiO_2-nylon interfacial interaction than that of nylon 6/SiO_2 and nylon 6/SiO_2-NH_2 nanocomposites. SEM analysis displays that all samples present a typical ductile fracture behavior. It can also find that SiO_2-COOH nanoparticles are homogeneously dispersed over the entire body of the nylon 6 matrix, which further confirms that SiO_2-COOH nanoparticles have good compatibility with nylon 6 matrix. The materials with high mechanical properties may be applied in plastic engineering area.

References

1. Hernández-Hernández, E.; Neira-Velázquez, M. G.; Mendez-Nonell, J.; Ramos-deValle, L. F. J Appl Polym Sci 2009, 112, 3510.
2. Hasan, M. M.; Zhou, Y. X.; Mahfuz, H.; Jeelani, S. Mater Sci Eng A 2006, 429, 181.
3. Qu, C.; Yang, H.; Liang, D.; Cao, W.; Fu, Q. J Appl Polym Sci 2007, 104, 2288.
4. Rusu, G.; Rusu, E. High Perform Polym 2006, 18, 355.
5. Li, Y.; Yu, J.; Guo, Z. X. J Appl Polym Sci 2002, 84, 827.
6. Cho, J. W.; Paul, D. R. Polymer 2001, 42, 1083.
7. Varlot, K. M.; Reynaud, E.; Vigier, G.; Varlet, J. J Polym Sci Part B: Polym Phys 2002, 40, 272.
8. Hasegawa, N.; Okamoto, H.; Kato, M.; Usuki, A.; Sato, N. Polymer 2003, 44, 2933.
9. Loo L. S.; Gleason, K. K. Polymer 2004, 45, 5933.
10. Dasari, A.; Yu, Z. Z.; Mai, Y. W.; Hu, G. H.; Varlet, J. Compos Sci Technol 2005, 65, 2314.
11. Ito, M.; Nagai, K. J Appl Polym Sci 2010, 118, 928.
12. Letuchi, M.; Tzur, A.; Tchoudakov, R.; Narkis, M.; Siegmann, A. Polym Compos 2007, 28, 417.
13. Kim, K. J.; Lee, J. S.; Prabu, A. A.; Kim, T. H. Polym Compos 2009, 30, 265.
14. Somwangthanaroj, A.; Ubankhlong, W.; Tanthapanichakoon W. J Appl Polym Sci 2010, 118, 538.
15. Gao, J. B.; Itkis, M. E.; Yu, A. P.; Bekyarova, E.; Zhao, B.; Haddon, R. C. J Am Chem Soc 2005, 127, 3847.
16. Gao, J. B.; Zhao, B.; Itkis, M. E.; Bekyarova, E.; Hu, H.; Kranak, V.; Yu, A. P.; Haddon, R. C. J Am Chem Soc 2006, 128, 7492.
17. Reynaud, E.; Jouen, T.; Gauthier, C.; Vigier, G.; Varlet, J. Polymer 2001, 42, 8759.
18. Yang, F.; Ou, Y. C.; Yu, Z. Z. J Appl Polym Sci 1998, 69, 355.
19. Mahalingam, V.; Onclin, S.; Peter, M.; Ravoo, B. J.; Huskens, J.; ReinHoudt, D. B. Langmuir 2004, 20, 11756.
20. Levy, L.; Sahoo, Y.; Kim, K. S.; Bergey, E. J.; Prasad, P. N. Chem Mater 2002, 14, 3715.
21. Rodriguez-Rios, H.; Nuno-Donlucas, S. M.; Puig, J. E.; Gonzalez-Nunez, R.; Schulz, P. C. J Appl Polym Sci 2004, 91, 1736.
22. Peng, B.; Tang, F. Q.; Chen, D.; Ren, X. L.; Meng, X. W.; Ren, J. J Colloid Inter Sci 2009, 329, 62.
23. Zhou, L.; Gao, C.; Xu, W. J. Langmuir 2010, 26, 11217.
24. Odian, G. Principles of Polymerization; New York: Wiley, 1991; Chapter 7.
25. Kruissink, C. A.; Van der Want, G. M.; Staverman, A. J. J Polym Sci 1958, 30, 67.

26. Heikens, D.; Hermans, P. H.; Van der Want, G. M. J Polym Sci 1958, 30, 81.
27. Heikens, D.; Hermans, P. H.; Van der Want, G. M. J Polym Sci 1960, 44, 437.
28. Shalaby, S. W.; Reimschuessel, H. K. J Polym Sci Polym Chem Ed 1977, 15, 1349.
29. Stehlicek, J.; Sebendinga, J. Eur Polym Mater 1986, 22, 5.
30. Zhang, Y.; Zhang, Q. L.; Cheng, K. L.; Xu, J. R. J Appl Polym Sci 2004, 92, 722.
31. Zhang, F.; Zhou, L.; Liu, Y. C.; Xu, W. J.; Xiong, Y. Q. J Appl Polym Sci 2008, 108, 2365.
32. Garcia, M.; Vliet, G. V.; Cate, G. J.; Chavez, F.; Norder, B.; Kooi, B.; Zyl, W. E.; Verweij, H.; Blank, D. H. Polym Adv Technol 2004, 15, 164.
33. Klabunde, K. J. Nanoscale Materials in Chemistry, 1st ed.; Wiley- Interscience: New York, 2001.
34. Zhang, B. Q.; Wong, J. S. P.; Shi, D.; Yam, R. C. M.; Li, R. K. Y. J Appl Polym Sci 2010, 115, 469.
35. Zhao, Z. D.; Yu, W. X.; Liu Y. H.; Zhang, J. Q.; Shao, Z. J Mater Lett 2004, 58, 802.
36. Moniruzzaman, M.; Chattopadhyay, J.; Billups, W. E.; Winey, K. I. Nano Lett 2007, 7, 1178.